

Determination of Optical Band Gap and Optical Constants of $\text{Ge}_x\text{Sb}_{40-x}\text{Se}_{60}$ Thin Films

M. M. Hafiz, N. El-kabany*, H. Mahfoz, Kotb and Y. M. Bakier.

Physics Department, Faculty of Science, Assiut University, Egypt.

Received: 21 Mar. 2015, Revised: 22 Jul. 2015, Accepted: 24 Jul. 2015.

Published online: 1 Sep. 2015.

Abstract: $\text{Ge}_x\text{Sb}_{40-x}\text{Se}_{60}$ (where $10 \leq x \leq 30$ at %) thin films were prepared on glass substrates by thermal evaporation technique. X-ray diffraction analysis for as-deposited films showed that they have amorphous structure. The optical constants of the as-deposited films were calculated from optical transmittance and reflectance data in wavelength range from 400 to 1200 nm. We found that both refractive index, n and extinction coefficient, k increased with increasing photon energy. Optical band gap was determined from absorption coefficient data using Tauc procedure and from the energetic distribution of the absorption coefficient. The optical absorption data indicate that the absorption mechanism is due to indirect transition. The optical gap of the as-deposited films was found to decrease monotonically with increasing Sb content, a result was interpreted on the basis of the chemical-bond approach. The dispersion of the refractive index is analyzed in terms of Wemple-DiDomenico single oscillator model. The optical dispersion parameters E_0 and E_d were determined according to this model. The characteristic Urbach's parameters such as steepness parameter, σ and Urbach's energy have been determined. The real and imaginary parts of the dielectric constant in addition to the dissipation factor $\tan \delta$ and the optical conductivity were also determined.

Keywords: Optical properties, Transmission spectrum, optical band gap, chalcogenide.

1 Introduction

Chalcogenide glassy semiconductors have several useful properties especially their applications in the fields of infrared optical elements, fiber optics and novel memory devices [1-4]. They also show a continuous change in the physical properties with change of chemical composition. Furthermore, several of these glasses are easily formed by quenching from melt over a wide compositional range, making them a suitable model systematic studied of various physical properties [5].

Optical absorption measurements are used to obtain the band structure and the energy gap of ternary chalcogenide amorphous thin films, because the analysis of the optical absorption spectra is one of the most productive tools for understanding and developing the energy band diagram of both crystalline and amorphous materials.

The importance of Ge-Sb-Se glasses is due to their interesting optical properties for their potential use as optical fibers, where they show high transparency to infrared radiation from 2 to 16 μm [6]. The glass forming region in the Ge-Sb-Se system extends from about 5 to 35 at % germanium, 5 to 40 at % antimony, the rest being selenium [7]. Physical properties of Ge-Sb-Se, as chalcogenide

semiconducting glasses, are strongly dependent on their composition [8,9] and hence, composition is of special importance in studying their physical properties. In the present work, samples of $\text{Ge}_x\text{Sb}_{40-x}\text{Se}_{60}$ ($x=10, 20$ and 30 at %) were prepared in the form of thin films. The optical properties deduced from optical transmittance and reflectance data at room temperature for as-deposited films were studied. The data are analyzed to determine the optical constants (refractive index n , absorption index k and absorption coefficient (α)). An analysis of the absorption coefficient has been carried out to obtain the optical band gap and determine the nature of the transitions involved. X-ray diffraction have been carried out to get an idea of the structure of $\text{Ge}_x\text{Sb}_{40-x}\text{Se}_{60}$ films.

2 Experimental

Chalcogenide glasses of $\text{Ge}_x\text{Sb}_{40-x}\text{Se}_{60}$ ($x=10, 20$ and 30 at %) were prepared by the melt-quenched technique. The high-purity elements were weighted according to their atomic percentages and were sealed in evacuated silica tubes, which were heated at 1200°C for 15h. The ampoules were frequently rocked at maximum temperature to insure the homogeneity of the melt. The quenching was performed in

*Corresponding author E-mail: Nahid_abuelhassan@yahoo.com

ice water. Thin films were prepared by thermal evaporation under vacuum of 10^{-5} Torr using an Edwards E-306 coating system. The evaporation rates as well as the film thickness were controlled by using a quartz crystal monitor FTM 5.

In order to determine the absorption coefficient α and the optical constants of the films as a function of the incident light wavelength, the transmittance $T(\lambda)$ and reflectance $R(\lambda)$ were recorded at room temperature using a double-beam spectrophotometer (Shimadzu UV-210 combined with PC)

The glassy nature of the prepared thin films was confirmed by XRD analysis using an X-ray diffractometer (Philips, PW 1710), with Cu as a target ($\lambda=1.54178\text{\AA}$), at 40kV and 30 mA with scanning speed 2° min^{-1} .

3 Results and Discussion

The X-ray diffraction patterns obtained for the investigated composition in the thin film form are shown in Fig.1.

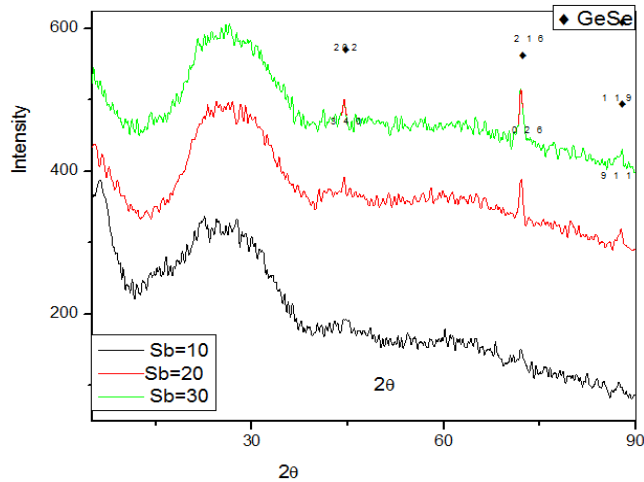


Figure 1: X-ray diffraction patterns of $\text{Ge}_x\text{Sb}_{40-x}\text{Se}_{60}$ thin films.

It is clear from this patterns that no sharp peak were observed at any of the recorded angles, indicates that $\text{Ge}_x\text{Sb}_{40-x}\text{Se}_{60}$ ($x=10, 20$ and 30 at %) are in amorphous state.

3.1 UV- visible spectroscopic studies

In order to study the effect of thin film composition on the optical properties, the transmission and reflectance spectra of thin films with different composition are shown in Figs 2 and 3 respectively. The UV- visible spectroscopy has been used in the spectral range (300-1200nm). Fig 2 shows the spectral distribution of the transmittance (T) for the as prepared samples of $\text{Ge}_x\text{Sb}_{40-x}\text{Se}_{60}$ thin films. It is noticed that the transmittance has low value at wavelength (500nm) and gradually rises towards longer wavelength and the peaks of transmittance reaches its maximum value at 975 nm for Sb content equal 30 at%. After that the transmittance decreases with increasing the wavelength. For shorter

wavelength, transmittance decreases rather quickly, and approaches near zero at around 300 nm. A sharp decrease toward UV region (below 350 nm) is due to the fundamental absorption of light caused by the excitation of electrons from valence band (VB) to conduction band (CB).

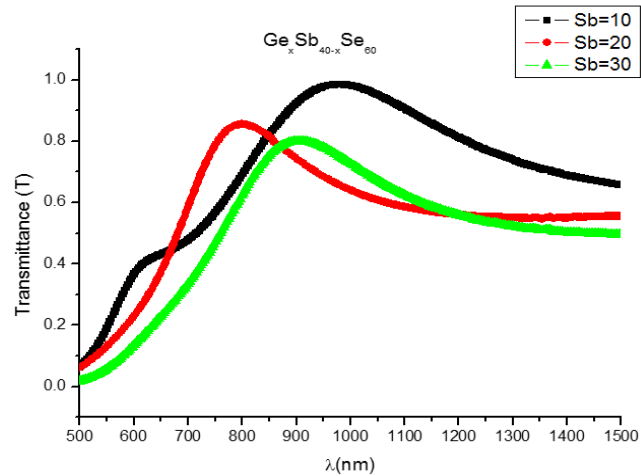


Figure 2: Transmittance spectra of $\text{Ge}_x\text{Sb}_{40-x}\text{Se}_{60}$ thin films as a function of wavelength.

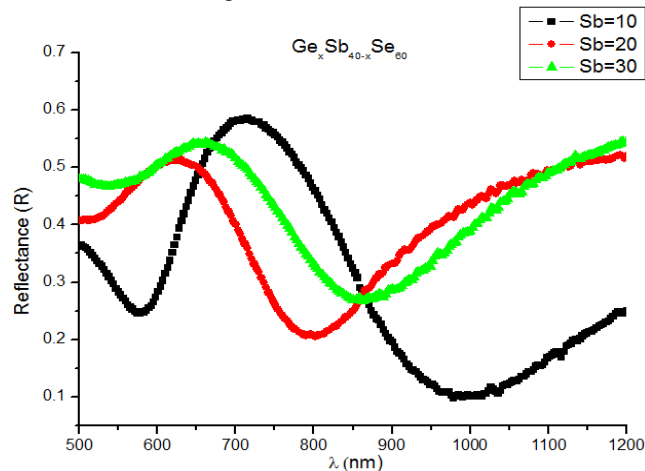


Figure 3: reflectance spectra of $\text{Ge}_x\text{Sb}_{40-x}\text{Se}_{60}$ thin films as a function of wavelength.

Similar type of behaviour is observed for the other samples.

3.2 Absorption coefficient and Tauc gap

The absorption coefficient (α) was computed from the experimentally measured values of transmittance $T(\lambda)$ and reflectance $R(\lambda)$ according to the following relation [10]:

$$T = (1-R)^2 \exp(-\alpha d) / [(1-R^2) \exp(-2\alpha d)] \quad (1)$$

Where, d (cm) is the film thickness. In chalcogenide glasses, a typical absorption edge can be broadly ascribed to either the three processes:

1) A high absorption region ($\alpha > 10^4 \text{ cm}^{-1}$), where assuming parabolic band edges and energy independent matrix

element for the inter-band transitions, the absorption coefficient (α) is given by Tauc relation [11]

$$(\alpha h\nu) = \beta (h\nu - E_{opt})^r \quad (2)$$

where β is the edge width parameter representing the film quality, E_{opt} is the optical energy gap of the material and r is a parameter characterizes the type of the optical transition process (direct or indirect) and the profile of electron density in valence and conduction bands.

2) An intermediate absorption range ($1\text{cm}^{-1} < \alpha < 10^4\text{cm}^{-1}$), in which the absorption depends exponentially on the photon energy and obey Urbach's empirical relation [12].

$$\alpha(\omega) = \alpha_0 \exp(h\nu / E_t) \quad (3)$$

With a slope parameter E_t , is Urbach energy which is interpreted as the width of band tails of localized states in the band – gap and in general represents the degree of disorder in an amorphous semiconductor [13]. The absorption in this region is due to transitions between extended states in one band and localized states in the exponential tail of the other band [14].

3) A weak absorption tail at low absorption constants ($\alpha < 1\text{cm}^{-1}$) whose shape and magnitude depends on the purity, thermal history, and preparation conditions.

In the region of low absorption, the absorption coefficient (α) shows an exponential dependence on the photon energy $h\nu$, and obeys Urbach's relation given in Eq (3).

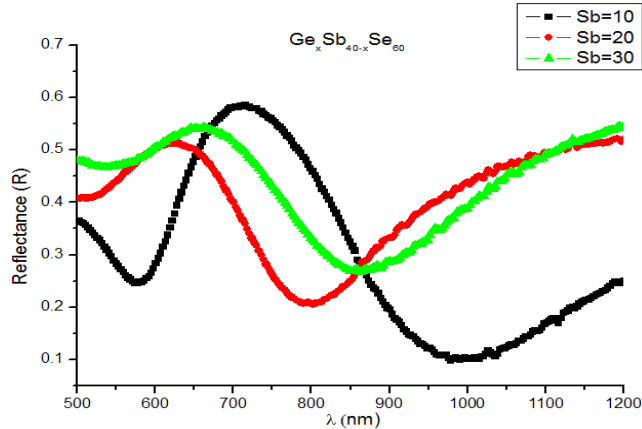


Figure 4: The relation between $\ln(\alpha)$ as a function of photon energy of $\text{Ge}_x\text{Sb}_{40-x}\text{Se}_{60}$ thin films.

Thus plotting of $\ln(\alpha)$ vs, $h\nu$, Fig.4 should give straight line with the inverse of its slope equals E_t . The calculated values of E_t for different film composition are given in Table.1. It is observed that E_t increases with increasing Sb content, this can be attributed to the process of deposition of atoms on the substrate, which may cause the formation of structural defects like unsatisfied bonds [15]. These structural defects increase as the Sb content increases. Therefore, isolated centers of these defects can only introduce states at or near the band edges leading to an increase in the band tail width values [16].

The dependence of $(\alpha h\nu)^{1/r}$ on photon energy ($h\nu$) is found to fit at $r=2$ for the investigated thin films indicates that, the absorption mechanism for $\text{Ge}_x\text{Sb}_{40-x}\text{Se}_{60}$ films is indirect transition. The optical band gap, E_g , for each composition was determined from the intercepts of the extrapolated linear part plots of $(\alpha h\nu)^{1/2}$ versus photon energy ($h\nu$) as shown in Fig.5. The obtained values of E_g , are given in Table.1, it is clear that the optical gap, E_g has the tendency to decrease with increasing Sb content.

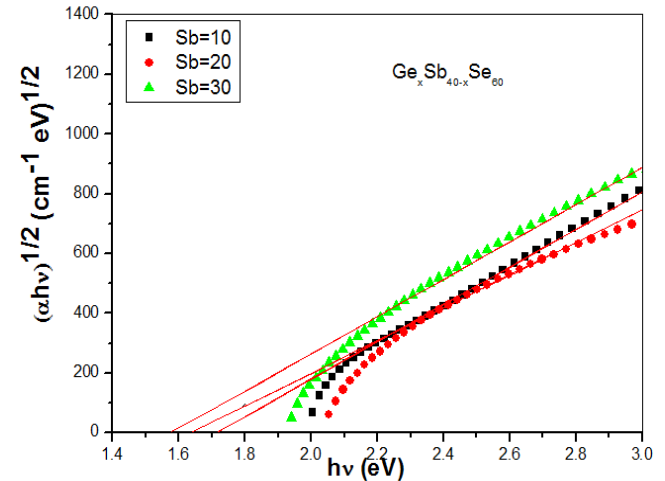


Figure 5: The relation between $(\alpha h\nu)^{1/2}$ as a function of photon energy of $\text{Ge}_x\text{Sb}_{40-x}\text{Se}_{60}$ thin films.

Table 1: The optical parameters of $\text{Ge}_x\text{Sb}_{40-x}\text{Se}_{60}$ thin films (Average coordination number $\langle r \rangle$), cohesive energy E_g , optical band gap, E_t the width of localized states, σ the steepness parameters.

Sb (at.%)	$\langle r \rangle$	C.E(ev)	$E_g(\text{eV})$	$E_t(\text{eV})$	σ
10	2.7	2.78	1.7165	0.296	0.0864
20	2.6	2.67	1.6624	0.333	0.0768
30	2.5	2.56	1.5853	0.3416	0.0749

The steepness parameter σ , characterizing the broadening of the optical absorption edge due to electron phonon or exciton- phonon interactions [17] was also determined taking $T=300\text{K}$ from the relation $\sigma = kT/E_t$. The values

of σ for different $\text{Ge}_x\text{Sb}_{40-x}\text{Se}_{60}$ thin films are given in Table .1. It is noticed that the steepness parameter σ has the same trend as the optical band gap.

It is clear from Table.1 that the optical energy gap E_g decreases, while the band tail width E_t increases with increasing the Sb content. This change in optical band gap may be discussed on the basis of the change in average bond energy as a function of composition. Since optical band gap is a bond sensitive property, a decrease in the average bond energy results in a decrease in the optical band gap [18]. According to the chemical – bond approach which assumes that, bonds are formed in sequence of decreasing bond energies until all available valences for the atoms are saturated [19]. The addition of Sb on Ge-Se must bring about a compositional change of host network of Ge-Se. The Sb atoms may be enter into Se chain resulting in the

systematical formation of Se-Sb bonds having bond energy of (51.15kcal/mol). Since the bond energy of Ge-Se (59.9) kcal/mol is higher than the bond energy of Se-Sb bond [20]. Decrease in the optical band gap with increasing Sb content is due to the formation of Se-Sb bonds having lower bond energy than Ge-Se bonds. Due to this low bond energy, the overall energy of the system decreases leads to the optical band gap decrease [21].

For more comprehension of the behavior of the optical gap with composition, the value of cohesive energy CE (average bond energy per atom) and average coordination number $\langle r \rangle$ (average number of covalent bonds per atom) for the investigated compositions were calculated. The cohesive energy of the studied compositions can be calculated using the chemical bond approach [22]. It is noticed that the values of CE and $\langle r \rangle$ vary exactly in the same manner as E_g , i.e, it decreases, with increasing Sb content. As illustrated in Table .1. The number of Ge-Se bonds decreases as the Sb content increases resulting in decrease in the cohesive energy of the Ge-Sb-Se system, this decrease, in turn, will lower the conduction band edge and thereby will decrease E_g [23].

Therefore, it can be concluded that the behavior of the optical band gap with increasing Sb content can also be interpreted in terms of the change in the values of the above mentioned parameters with composition.

3.3 Dispersion behavior of refractive index

The refractive index (n) of the films at different compositions are determined from the transmittance and reflectance spectra of the thin films.

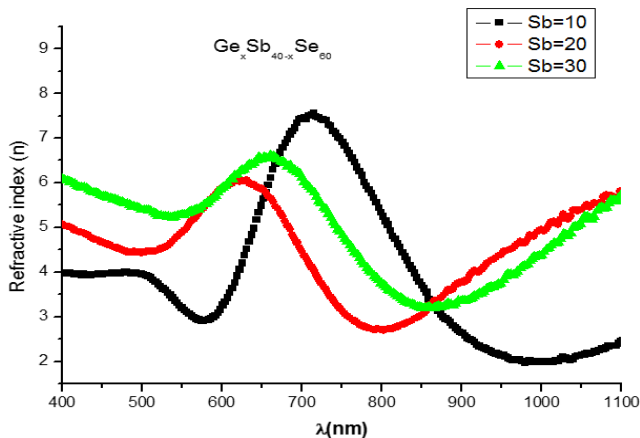


Figure 6: Refractive index of $Ge_xSb_{40-x}Se_{60}$ thin films. As a function of wavelength.

The reflectance spectra of the thin films exhibit a peak at energies to the interband transitions. The spectral curves of n values determined using the following relation

$$R = \frac{\{(n-1)^2 + k^2\}}{\{(n+1)^2 + k^2\}} \quad (4)$$

Where R is the reflectance and k is the extinction coefficient, which also called absorption index is a measure of the fraction of light lost due to scattering and absorption per unit distance of the participating medium. The extinction coefficient has been calculated using the relation [24-27].

$$k = \frac{\alpha\lambda}{4\pi}$$

The dependence of refractive index, n and extinction coefficient, k of $Ge_xSb_{40-x}Se_{60}$ thin films on the wavelength λ are shown in Fig 6 and 7. Both refractive index and extinction coefficient for the thin films under investigation have been found to decreases with increases the wavelength. It is noticed that a peak is observed in the refractive index spectra of the compound and shifts toward higher photon energies.

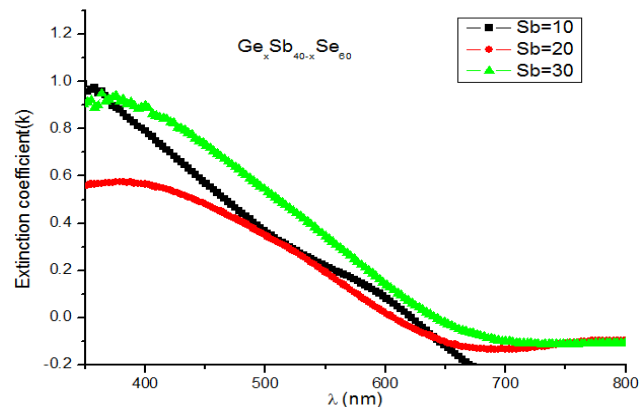


Figure 7: The extinction coefficient (k) as a function of wavelength for $Ge_xSb_{40-x}Se_{60}$ thin films.

The decrease of extinction coefficient with the increase of wavelength indicates that the fraction of light lost due to scattering and absorbance decreases. It is obvious that, the extinction coefficient at each composition has the tendency to increase towards lower wavelengths corresponding to the beginning of strong electronic absorption.

3.4 Dispersion energy, oscillator strength and static refractive index from Wemple- Di-Domenico model

The obtained data for the refractive index (n) can be analyzed by using the Wemple- Di-Domenico (WDD) model which is based on single effective oscillator approach in the region from ultraviolet to near - infrared. The high frequency properties of thin films under investigation could be treated as single oscillator.

According to single oscillator model proposed by WDD [28,29], The relation between the refractive index, n and the single oscillator strength below the band gap is given by the following expression:

$$n^2(h\nu) = 1 + \frac{E_o E_d}{E_o^2 - (h\nu)^2} \quad (5)$$

where E_0 and E_d are single oscillator constants, which represented by the energy of the effective dispersion oscillator and the dispersion energy, respectively, which measures the average strength of interband optical transitions. Fig.8 illustrates the plotting of $(n^2-1)^{-1}$ versus $(h\nu)^2$ for the investigated films, yields a straight line for normal behavior having the slope $(E_0E_d)^{-1}$ and the intercept with the vertical axis is E_0/E_d from which E_0 and E_d can be directly determined[29].

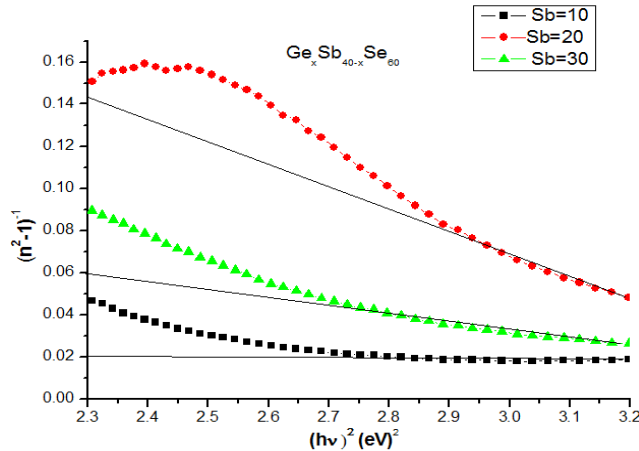


Figure 8: A plot of $(n^2-1)^{-1}$ versus $(h\nu)^2$ for $Ge_xSb_{40-x}Se_{60}$ thin films.

Table 2: The parameters ϵ_∞ , N/m^*E_0 , the oscillator energy, E_d , the dispersion energy and n_0 is the static refractive index for $Ge_xSb_{40-x}Se_{60}$ thin films.

Sb (at.%)	ϵ_∞	$N/m^*(m^{-3}Kg^{-1})$	$E_0(eV)$	$E_d(eV)$	n_0
10	16.553	1.849×10^{51}	2.1889	21.585	3.296
20	29.765	3.6236×10^{51}	2.0409	7.0529	2.111
30	38.112	5.431×10^{51}	1.9917	10.157	2.469

The obtained values of the parameters E_0 and E_d are given in Table.2, the material parameters, E_0 and E_d , give average features of the oscillators. It is observed that the variation in the transition strength, E_d , results primarily from changes in the nearest neighbour coordination number.

The values for the static refractive index n_0 have been calculated from WDD dispersion parameters E_0 and E_d by using the formula

$$n_0 = \left(1 + \frac{E_d}{E_0}\right)^{1/2} \quad (6)$$

The values of n_0 are calculated by extrapolating the WDD dispersion equation to $h\nu \rightarrow 0$ (Eq.(5)). The values of n_0 are given in Table.2.

3.5 Determination of the complex dielectric constant near the absorption edge

The obtained data of refractive index (n) can be analyzed to obtain the high frequency dielectric constant (ϵ_∞) via the following procedure [30]. This procedure describes the

contribution of the free carriers and the lattice vibrational modes of the dispersion.

The complex refractive index $\hat{n} = n + ik$ and complex dielectric constant $\hat{\epsilon} = \epsilon_1 + i\epsilon_2$ characterize the optical properties of any solid material. The real and imaginary parts of the dielectric constants ϵ_1 and ϵ_2 of the investigated films (in the absorption region) were also determined by the following relation [31]:

$$\epsilon_1 = n^2 - k^2 = \epsilon_\infty - \left(\frac{e^2 N}{4\pi^2 c^2 \epsilon_0 m^*}\right) \lambda^2 \quad (7)$$

And

$$\epsilon_2 = 2nk = \left(\frac{\epsilon_\infty \omega_p^2}{8\pi^2 c^3 \tau}\right) \lambda^3 \quad (8)$$

where ϵ_1 is the real part of dielectric constant, ϵ_∞ is the lattice dielectric constant, λ is the wavelength, e is the charge of the electron, N is the free charge-carrier concentration, ϵ_0 is the permittivity of free space, m^* the effective mass of the electron and c the velocity of light.

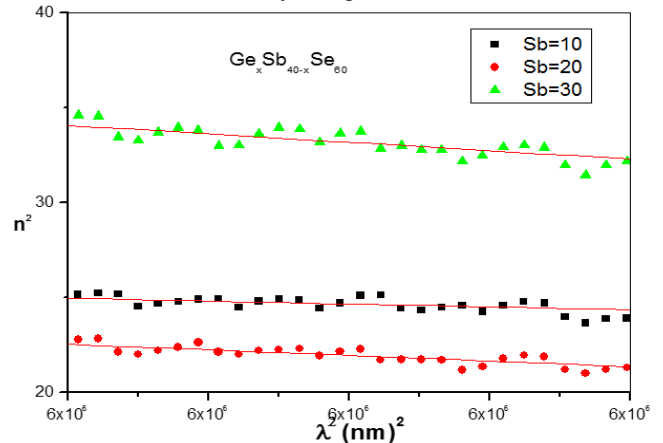


Figure 9: A plot of n^2 vs λ^2 for $Ge_xSb_{40-x}Se_{60}$ thin films.

It is observed that the dependence of $\epsilon_1 = n^2$ on λ^2 is linear at longer wavelength, as shown in Fig.9. Extrapolating the linear part of this dependence to zero wavelengths gives the value of ϵ_∞ and from the slopes of these lines we can calculate the values of N/m^* for the investigated compositions.

The values of ϵ_∞ and N/m^* are given in Fig.10 and 11 shown the dependence of the real and imaginary parts of the dielectric constant ϵ_1 and ϵ_2 with the photon energy $h\nu$ for all investigated film. It is seen that the values of ϵ_1 are higher than that of ϵ_2 . The variation of the dielectric constant with the photon energy indicates that some interactions between photons and electrons in the films are produced in this energy range. These interactions are observed on the shapes of the real and imaginary parts of the dielectric constant and they cause the formation of peaks in the dielectric spectra which depends on the material type. The

maximum peak height of these peaks corresponds to plasma frequency.

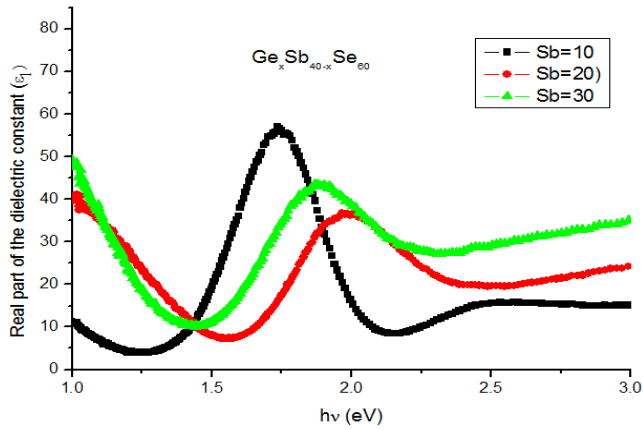


Figure 10: The variation of ϵ_1 with the photon energy for $\text{Ge}_x\text{Sb}_{40-x}\text{Se}_{60}$ thin films.

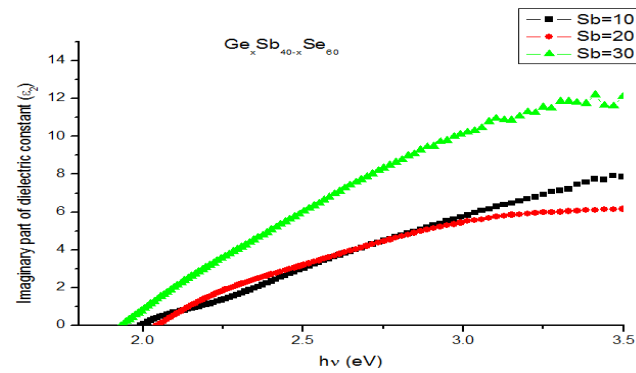


Figure 11: The relation between ϵ_2 with $h\nu$ for $\text{Ge}_x\text{Sb}_{40-x}\text{Se}_{60}$ thin films.

3.5.1 Determination of the optical conductivity

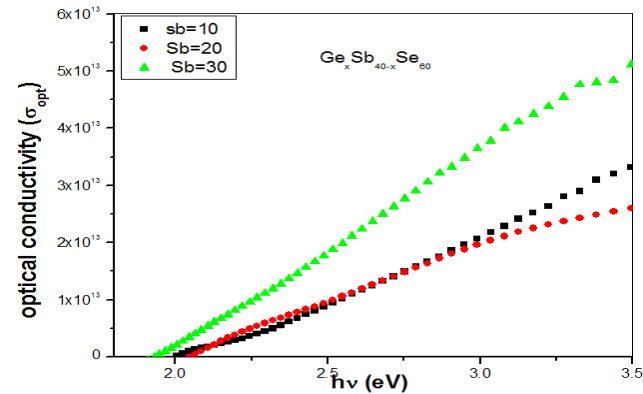


Figure 12: Plot of optical conductivity (σ_{opt}) versus with $h\nu$ for $\text{Ge}_x\text{Sb}_{40-x}\text{Se}_{60}$ thin films.

The absorption coefficient α can be used to calculate the optical conductivity (σ_{opt}) which can be determined from the relation [32]

$$\sigma_{opt} = \frac{\alpha n c}{4\pi} \tag{8}$$

Where c is the velocity of light, α is the absorption coefficient and n is the refractive index. The optical conductivity directly depends on the absorption coefficient and refractive index of the material and follow the same trend as the absorption coefficient and refractive index with increasing wavelength. Fig.12 shows the plot of optical conductivity versus photon energy for thin films under investigation. The increases of optical conductivity at high photon energies is due to the high absorbance of sample thin films and also may be due to the electron excited by photon energy [19]. It is noticed that the optical conductivity increases with increasing Sb content and has higher values for $\text{Ge}_{10}\text{Sb}_{30}\text{Se}_{60}$ thin film.

3.5.2 Determination of the dissipation factor tan δ

The dissipation factor (loss tangent) $\tan \delta$ can be calculated according to the following equation [33]:

$$\tan \delta = \frac{\epsilon_2}{\epsilon_1}$$

The variation of the dissipation factor of the investigated films with photon energy is shown in Fig 13.

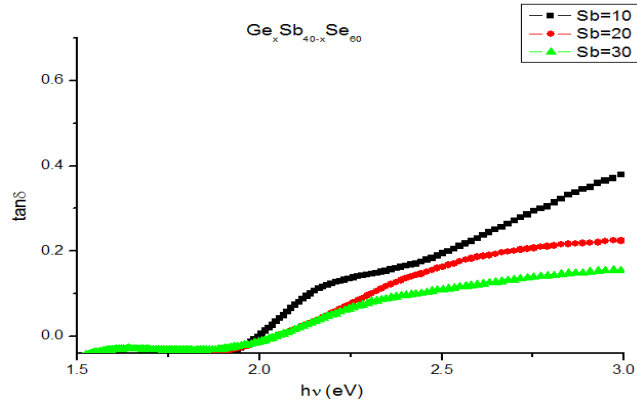


Figure 13: Dependance of the dissipation factor $\tan \delta$ on the photon energy for $\text{Ge}_x\text{Sb}_{40-x}\text{Se}_{60}$ thin films.

It is found that $\tan \delta$ increases with increasing photon energy and decreases with increasing Sb content.

4 Conclusion

The optical absorption measurements for $\text{Ge}_x\text{Sb}_{40-x}\text{Se}_{60}$ thin films were carried out in the UV/Visible region (300-700nm). It was found that the transmission spectra increases with increasing wavelength, while the reflectance decreases. On the basis of the optical investigations of the films, the following results were obtained.

- The type of optical transition responsible for optical absorption was indirect transition.

- The value of the optical gap decreases monotonically while the band tail width increases with increasing Sb content.
- The optical constants were analyzed from the transmittance and reflectance spectra. WDD model has been used to estimate the dispersion parameters E_0 and E_d .
- Both real and imaginary parts of dielectric constants were determined and the values of real part were higher than those of imaginary part. The optical conductivity has been found to increase with increasing Sb content and have higher values for $\text{Ge}_{10}\text{Sb}_{30}\text{Se}_{60}$ thin film.
- The dissipation factor decreases with increasing Sb content.

References

- [1] K. Abe, H. Takebe, K. Morinaga, J. Non-Cryst. Solids 212(1997)143
- [2] D. R. Simons, A. J. Faber, H. de Waal, J. Non-Cryst. Solids 185(1995)283
- [3] R. Zallen, the Physics of Amorphous Solids, Wiley, New York, 1983
- [4] N. F. Mott, E. A. Davis, Electronic process in Non-Crystalline Materials, Oxford University Press, Oxford, 1979
- [5] Mehra RM, Kumar R, Mathur PC, Shimakawa K, Philos Mag B 58(1988) 293
- [6] M. Frumer, H. Ticha, J. Klikorka and P. Tomiska, J. Non-Crystalline Solids 16(1975)175
- [7] Y. L. A. El-kady, Physica B 275(2000)344
- [8] Mott NF, Davis EA, Electronic processes in non- crystalline materials, Oxford: Clarendon Press; 1979
- [9] Davis EA, Electronic and structural properties of amorphous semiconductors. London/ New York: Academic Press; 1973[P.425]
- [10] M. Becker, H. Yfan, Phy.Rev.76 (1949)1530
- [11] J. Tauk, R. Grigorovici, A. Vancu, Phy. Sta. Solidi 15(1966)627
- [12] F. Urbach, Phys. Rev, 92(1953)132
- [13] J. A. Olley, Solid State Commun, 13(1973)1437
- [14] M. Suzuki, H. Ohdaira, T. Matsuni, M. Kumeda, T. Shimizu, J. Appl, Phys, 16(1977)221
- [15] Pamukchiev V, Levi Z, Savova E. Semicond Sci Technol 121 (1998)1390
- [16] O Reilly EP, Robertson J. Phy Rev B 34 (1986)8684
- [17] H.Mahr, Phys.Rev, 125(1962)1510
- [18] A. K. Pattanaik, A. Srinivasan, J. Optoelectron, Adv. Mater, 5 (2003) 1161
- [19] J. Bicerno, S. r. Ovshinsky, J. Non-Cryst. Solids 74(1985)75
- [20] M.Fadel, IndianJ.Pure Appl.Phys.37 (1999)57
- [21] T. Shimizu, I. Watanabe, M. Kumeda, and M. Ishikawa, J. Non-Cryst. Solids 35& 36,895(1980)
- [22] Fouad SS, Physica B 215(1995)213
- [23] Pamukchieva V, Szekeres A,Savova E,Vlaikova E,J.Non-Cryst Solids 242(1998)110
- [24] D. P. Gosain, T. Shimizu, M. Suzuki, T. Bando, S. Okano, J. Mater Sci.26 (1991)3271
- [25] N. Sharoff, A. K. Chakravati, Opt. Memories Technol- ogies and .Appl. 7(1991)83
- [26] D. J. Gravesteyn, Appl.Opt.27 (1988)736
- [27] E. K. Shokr, M. M. Wakhad, J.Mater.Sci.27 (1992)1197
- [28] M. Didomenico, S. H. Wemple, J. Appl, Phys, 40(1969)720
- [29] S. H. Wemple, M. Didomenico, Phys.Rev.B.3 (1971)1338
- [30] M. Baleva, E. Goranova, V. Darakchieva, S. Kossionides, M. Kokkosis, P. Jordanov, Vacuum, 69(2003) 425
- [31] F. Abeles(Ed), Optical properties of solids, North- Holland Publishing Company, Amsterdam, London, 1972
- [32] J.I.Pankove, Optical Processes in Semiconductors, Dover Publications Inc, New.York, 1975, pp.91
- [33] E. Yakuphanoghlu, A. Cukurovali, I. Yilmaz, Physica B.351 (2004)153